Participation of Histidine-51 in Catalysis by Horse Liver Alcohol Dehydrogenase[†,‡]

Laurie A. LeBrun,[§] Doo-Hong Park,[∥] S. Ramaswamy, and Bryce V. Plapp*

Department of Biochemistry, The University of Iowa, Iowa City, Iowa 52242

Received November 23, 2003; Revised Manuscript Received January 12, 2004

ABSTRACT: Histidine-51 in horse liver alcohol dehydrogenase (ADH) is part of a hydrogen-bonded system that appears to facilitate deprotonation of the hydroxyl group of water or alcohol ligated to the catalytic zinc. The contribution of His-51 to catalysis was studied by characterizing ADH with His-51 substituted with Gln (H51Q). The steady-state kinetic constants for ethanol oxidation and acetaldehyde reduction at pH 8 are similar for wild-type and H51Q enzymes. In contrast, the H51Q substitution significantly shifts the pH dependencies for steady-state and transient reactions and decreases by 11-fold the rate constant for the transient oxidation of ethanol at pH 8. Modest substrate deuterium isotope effects indicate that hydride transfer only partially limits the transient oxidation and turnover. Transient data show that the H51Q substitution significantly decreases the rate of isomerization of the enzyme−NAD^+ complex and becomes a limiting step for ethanol oxidation. Isomerization of the enzyme−NAD^+ complex is rate limiting for acetaldehyde reduction catalyzed by the wild-type enzyme, but release of alcohol is limiting for the H51Q enzyme. X-ray crystallography of doubly substituted His51Gln:Lys228Arg ADH complexed with NAD^+ and 2,3- or 2,4-difluorobenzyl alcohol shows that Gln-51 isosterically replaces histidine in interactions with the nicotinamide ribose of the coenzyme and that Arg-228 interacts with the adenosine monophosphate of the coenzyme without affecting the protein conformation. The difluorobenzyl alcohols bind in one conformation. His-51 participates in, but is not essential for, proton transfers in the mechanism.

Histidine-51 is thought to contribute to the acid/base catalysis of alcohol dehydrogenases (*1*−*6*). In structures of the horse and human liver enzymes, His-51 is part of a hydrogen-bonded system that connects the hydroxyl group of a water or an alcohol ligated to the catalytic zinc through the hydroxyl group of Ser-48 with the 2′-hydroxyl group of the nicotinamide ribose (*2*, *6*, *7*). During alcohol oxidation, this system could relay a proton to solvent, producing the alkoxide intermediate (Scheme 1), which would be oxidized by NAD^+. An inverse solvent isotope effect on the hydrogen transfer step suggests that the alkoxide is stabilized by a low barrier hydrogen bond to the serine hydroxyl group (*8*, *9*). Recent computational studies support the proposed mechanism (*10*, *11*), but the magnitude of the contribution of His-51 to the chemical steps has not been established.

Chemical modification of histidine residues with diethyl pyrocarbonate inactivated both horse and yeast ADH[1] (*3*, *12*). Substitution of His-51 with glutamine by site-directed mutagenesis in both yeast and human ADH1B ($\beta_1\beta_1$) moderately affects activity (*4*, *5*). Glutamine is nearly isosteric with histidine and can form hydrogen bonds with the nicotinamide ribose, but evidence for such structural flexibility is lacking. The H51Q substitution in yeast ADH decreased catalytic efficiency for ethanol oxidation (V_1/E_tK_b) by 30-fold at pH 7 and significantly altered the pH dependence (*4*). The H51Q substitution in human ADH1B shifted the pK values for trifluoroethanol and caprate inhibition from 7.8 for wild-type enzyme to 8.5 and decreased catalytic efficiency for ethanol oxidation by 6-fold at pH 7 (*5*). These studies support a role for His-51 as a general base.

Scheme 1

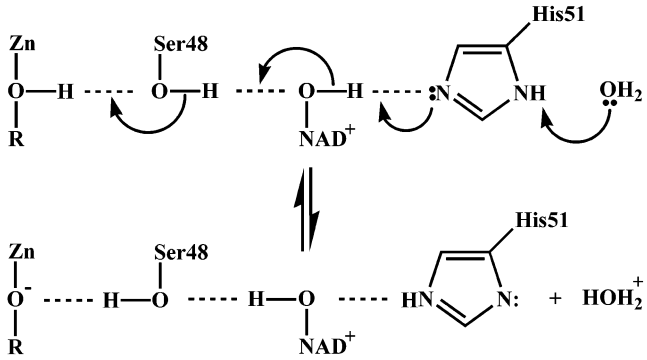

However, the effects of the H51Q substitutions are modest, suggesting to some that His-51 is not important for catalysis,

[†] This work was supported by National Science Foundation Grants MCB91-18657 and MCB95-06831 and NIH Grant AA00279.

[‡] The X-ray coordinates and structure factors have been deposited in the RCSB Protein Data Bank with entry names 1QV6 for the Q51R228 (His51Gln:Lys228Arg) alcohol dehydrogenase complexed with NAD^+ and 2,4-difluorobenzyl alcohol and 1QV7 for the complex with NAD^+ and 2,3-difluorobenzyl alcohol.

* Address correspondence to this author at the Department of Biochemistry, 4-370 Bowen Science Building, The University of Iowa, Iowa City, IA 52242-1109 (tel, 319-335-7909; fax, 319-335-9570; e-mail: bv-plapp@uiowa.edu).

[§] Current address: Anadys Pharmaceuticals, Inc., 6777 Nancy Ridge Drive, San Diego, CA 92121.

[∥] Current address: Director, Mogam Biotechnology Research Institute, 341 Pojung-ri, Koosung-eup, Yongin-si, Kyonggi-do 449-913, Korea.

[1] Abbreviations: ADH, liver alcohol dehydrogenase; H51Q, His-51 substituted with Gln; K228R, Lys-228 substituted with Arg; Q51R228, double mutant with H51Q and K228R substitutions; rmsd, root-mean-square deviation.

10.1021/bi036103m CCC: $27.50
Published on Web 02/14/2004

even though expectations should have an experimental basis (*13*). Furthermore, many homologous ADHs have Thr, Tyr, or Asn at the position corresponding to His-51 (*14*, *15*), indicating that His-51 is not absolutely essential. Substitution of Thr-51 in human ADH2 ($\pi\pi$ enzyme) with His decreases (rather than increases) by 3-fold catalytic efficiency with ethanol (*16*). Small changes in activity found with site-directed mutations might be explained by effects on the overall structure of the enzyme or by local changes in the hydrogen-bonded system. Of course, changes in steady-state kinetic parameters may not reveal the extent of participation of a residue in critical steps in the mechanism. To measure the contribution of His-51 to catalysis requires structural studies, steady-state and transient kinetics, pH dependencies, and isotope effects, which together provide a comprehensive analysis of the participation of His-51 in the various steps in the mechanism.

We prepared the H51Q, K228R, and Q51R228 enzymes previously and found that the steady-state kinetic constants (*K* values) for ethanol oxidation and acetaldehyde reduction measured at pH 8 for H51Q ADH change less than 3-fold, whereas those for K228R ADH increase on average about 4-fold, and those for Q51R228 ADH increase about 15-fold (*17*). Lys-228 participates in binding of the adenosine monophosphate moiety of the coenzyme, and some effects of the K228R substitution on coenzyme binding are expected (*6*). Maximum velocities for the forward and reverse reactions change modestly, up to 3-fold, but dissociation of coenzyme is predominantly rate limiting for turnover. Transient data show that the H51Q substitution significantly affects, in a similar way for both H51Q and Q51R228 ADHs, the rate constants and pH dependence for the binding of NAD^+ as compared to the wild-type enzyme (*17*). The effects were attributed to the contribution of His-51 in deprotonating the catalytic zinc-bound water and the isomerization of the enzyme$-NAD^+$ complex. The K228R substitution also affects binding of NAD^+ but produces a different pH dependence. To assess further the modulating effect of His-51 on catalysis, we examined various steps of the mechanism of H51Q ADH, where the role of the catalytic zinc can be studied. We also determined structures, at 1.8 Å resolution, of ternary complexes of the Q51R228 ADH with NAD^+ and the substrate analogues 2,3-difluorobenzyl or 2,4-difluorobenzyl alcohols. The results show how the enzyme can accommodate the H51Q and K228R substitutions, which is relevant to the study on coenzyme binding (*17*) and the present work. In addition, the structures show how alcohols bind in the hydrogen-bonded system with Gln-51 and how the enzyme recognizes fluorinated substrates.

EXPERIMENTAL PROCEDURES

Materials. $LiNAD^+$ (grade I) and Na_2NADH (grade I) were obtained from Roche Molecular Biochemicals. Isotopically labeled substrates (ethanol-d_6, 1-propanol-1,1-d_2, 1-butanol-d_9, cyclohexanol-d_{12}, and benzyl alcohol-α,α-d_2) and D_2O were purchased from MSD Isotopes, Inc.

Mutagenesis. The plasmid pBPP/ADH-E/H51Q was created by site-directed mutagenesis with the Amersham mutagenesis kit, version 2, starting with the plasmid pBPP containing the cDNA for the horse E isoenzyme (*18*). The oligodeoxyribonucleotide, 5′-CA GAT GAC CAG GTG GTT AG-3′ (mutation site is underlined), was used as the primer for mutagenesis of pBPP/ADH-E/H51Q. The mutations were confirmed by restriction mapping and DNA sequencing of the complete coding region.

Purification. The mutated enzymes were purified by the procedure previously described (*17*, *18*) and appeared to be homogeneous by the criterion of polyacrylamide gel electrophoresis in the presence of sodium dodecyl sulfate. The concentration of active enzyme sites (N, normality) for the purified enzymes was determined by titration with NAD^+ in the presence of pyrazole (*19*). Automated Edman degradation of the intact protein showed that amino-terminal sequence Ser-Thr-Ala-Gly-Lys-Val-Ile-Lys was obtained in good yield and thus was not acetylated, in contrast to the acetylated enzyme that is isolated from horse liver (*20*).

Steady-State Kinetics. Initial velocities of the enzyme activity were determined by measuring the change in absorbance at 340 nm with a Cary 118C spectrophotometer interfaced to a computer with a Data Translation 2805 A/D board. An SLM fluorometer (model 4800 C) was also used with excitation at 340 nm and emission at 460 nm. Data were collected by using a computer interfaced to the fluorometer. Initial velocities were estimated by a linear or parabolic fit of the data. The kinetic constants were calculated with the programs from Cleland (*21*).

Transient Kinetics. Transient kinetics were studied with the BioLogic SFM3 stopped-flow instrument, which allows concentrations of substrates to be varied systematically with three syringes. The dead time of the instrument was 2.3 ms. The transient data were collected at 25 °C and analyzed with the BioKine software. The transient curves were best fit to a single exponential process by the equation $A_t = A_0 \exp(-k_1 t) +$ baseline, where A_t is the absorbance at time t, A_0 is the maximum absorbance change, k_1 is the observed rate constant, and t is time.

The transient reactions for the oxidation of ethanol and the reduction of acetaldehyde were followed by the change in absorbance at 333 nm ($\epsilon = 5.5\ mM^{-1}\ cm^{-1}$), which is near the isosbestic point for free and enzyme-bound forms of NADH (*22*). The kinetic simulation program KINSIM and the automatic fitting routine FITSIM (*23*) were used to estimate the rate constants from the transient progress curves collected with the BioLogic instrument by fitting several progress curves simultaneously.

pH Dependence Studies. Buffers of 10 mM $Na_4P_2O_7$, 0.25 mM EDTA, and sufficient H_3PO_4, NaH_2PO_4 and Na_2HPO_4 to produce the desired pH and a final ionic strength of 0.1 were used in the pH range of 5.5−9.5 (*24*). Buffers at pH 9.5 or above had a final concentration of 10 mM $Na_4P_2O_7$, 0.25 mM EDTA, and 5 mM sodium carbonate. The buffers were made as double strength and diluted 2-fold in the final reaction mixture with enzyme in weakly buffered solutions. The p*K* values for the pH dependencies were determined by fitting the data with an iterative nonlinear least squares program [NONLIN, from C. M. Metzler, The Upjohn Co., or from M. L. Johnson (*25*)] to equations derived for various mechanisms of ionization (*26*).

A general mechanism with three ionizable groups that can describe the pH dependencies is shown is Scheme 2. Equation 1 describes a mechanism with a single ionizable group where only the unprotonated form is active. Equation 2 describes a mechanism with one ionizable group, and only

Scheme 2

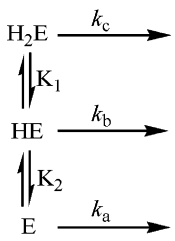

the protonated form of the enzyme reacts. Equation 3 describes a mechanism that involves two ionizable groups, and only the monoprotonated form is active. Equation 4 describes a mechanism with one ionizable group where both forms are active, and the unprotonated form is most active. Equation 5 describes a mechanism with two ionizable groups where both the monoprotonated and unprotonated forms can react; the unprotonated form is most reactive. Equation 6 describes a mechanism with two ionizable groups where each enzyme form has finite activity, and the unprotonated form is most active. For binding of competitive inhibitors, the k_{obs} is replaced with $1/K_d$ (the binding constant) and the k_x with $1/K_{d,max}$ so that the pH-independent binding constant and the pK for the enzyme form to which the inhibitor binds are obtained.

$$k_{obs} = k_a/(1 + [H^+]/K_2) \quad (1)$$

$$k_{obs} = k_b/(1 + K_2/[H^+]) \quad (2)$$

$$k_{obs} = k_b/(1 + [H^+]/K_1 + K_2/[H^+]) \quad (3)$$

$$k_{obs} = (k_b + k_aK_2/[H^+])/(1 + K_2/[H^+]) \quad (4)$$

$$k_{obs} = (k_b + k_aK_2/[H^+])/(1 + [H^+]/K_1 + K_2/[H^+]) \quad (5)$$

$$k_{obs} = (k_a[H^+]/K_2 + k_b + k_cK_1/[H^+])/(1 + K_1/[H^+] + [H^+]/K_2) \quad (6)$$

X-ray Crystallography. Crystals of the doubly mutated Q51R228 enzyme (*17*) were produced by dialysis of 10 mg/mL enzyme in 50 mM ammonium *N*-[tris(hydroxymethyl)-methyl]-2-aminoethanesulfonate buffer, pH 7.0, at 5 °C (pH 6.7 at 25 °C), with 1 mM NAD^+ and 10 mM 2,3-difluorobenzyl alcohol or 2,4-difluorobenzyl alcohol, against gradually increasing concentrations of 2-methyl-2,4-pentanediol. Crystals formed at about 12% 2-methyl-2,4-pentanediol, and the concentration was finally raised to 25%. The crystals were thin rods, about 0.1 mm in the longest direction. Crystals were flash frozen, and data were collected at 100 K. A data set for the complex with 2,4-difluorobenzyl alcohol was collected from a single crystal at the ID14-EH4 beamline (using an ADSC CCD detector) at the ESRF in Grenoble, France. The data were processed using the program MOSFLM (*27*) and scaled using the program SCALA (*28*). Data for the complex with 2,3-difluorobenzyl alcohol were collected on the synchrotron in Lund, Sweden, using the MAR345 detector and were processed and scaled using XDS (*29*).

The structures were solved by molecular replacement using AMORE (*30*) and a starting model with coordinates for a dimer of the refined structure of the wild-type ADH complexed with NAD^+ and 2,3,4,5,6-pentafluorobenzyl alcohol (PDB entry 1hld) after removal of the waters and pentafluorobenzyl alcohol and with residues 51 and 228 mutated to alanines (*6*). The initial maps clearly showed electron density for many waters, the difluorobenzyl alcohol, and the side chains for glutamine at residue 51 and arginine at residue 228. The structures were refined by cycles of model building with O (*31*) and least squares refinement with the program REFMAC (*32*). Waters were added automatically using the program ARP (*33*) and confirmed by inspection. The structure of the complex with 2,3-difluorobenzyl alcohol was refined similarly, starting with the model for the 2,4-difluorobenzyl alcohol. The structures were evaluated with Procheck (*33*) and found to have parameters consistent with other high-resolution structures. Figures were made with the MolRay interface to the POV-ray tracer (*34*) with final electron density maps ($2F_o - F_c$) calculated at one standard deviation above the mean density.

RESULTS

pH Dependence of Kinetic Constants for the H51Q Enzyme. Steady-state and transient kinetics were used to determine the pH dependencies for various reactions of the H51Q enzyme over the pH range of 6−10 and were compared to the reactions for the wild-type enzyme (Figure 1). In principle, the pH dependencies reflect ionization of a group (or groups) that is involved in catalysis, but the kinetic complexity of the mechanism can shift pK values from the intrinsic values (*35*). Therefore, kinetic parameters for different reactions were determined so that different steps in the mechanism could be studied. For purposes of comparison, the results are grouped so that kinetics for the forward reaction are on the left side and the kinetics for the reverse reaction are on the right side for Figure 1A−F. Transient reactions relating to ethanol oxidation and NAD^+ binding are presented in Figure 1G,H. Fits of the data to the appropriate equations are given in Table 1.

The H51Q substitution significantly affects both the observed pK values and the magnitudes of the pH-independent kinetic parameters ("limiting values" in Table 1). Of particular interest, the pH dependence of the catalytic efficiency of ethanol, V_1/E_tK_b, which reflects the apparent pK value for the binary enzyme−NAD^+ complex, has been shifted to a value of 8.4 from the value of 6.7 for the low pH range of the dependence for the wild-type enzyme (Figure 1A). The binding of the competitive inhibitor trifluoroethanol, $1/K_{d,TFE}$, to the H51Q enzyme exhibited a pH dependence with a pK value of 8.5, which is shifted up from the value of 7.6 for the wild-type enzyme (Figure 1C). The similar pK values for V_1/E_tK_b and $1/K_{d,TFE}$ suggest that the intrinsic pK of the H51Q ADH−NAD^+ complex is about 8.5. The pK value for trifluoroethanol binding was also shifted from the value of 7.8 for the human ADH1B enzyme to 8.5 by the H51Q substitution (*5*).

The pH dependence for the steady-state turnover (V_1/E_t) is also altered by the H51Q substitution. The weak pH dependence of V_1/E_t for wild-type ADH over the pH range of 6−10 is controlled by release of the product NADH (*37*), whereas the H51Q enzyme has a complex dependence with pK values of 7.6 and 9.3, suggesting a change in the rate-limiting step for turnover (Figure 1E).

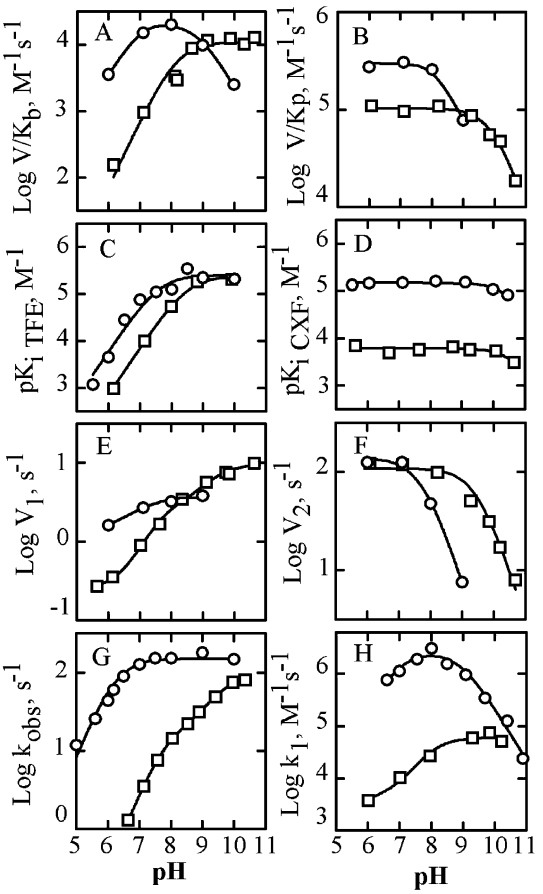

FIGURE 1: pH dependencies for reactions catalyzed by wild-type and H51Q enzymes. Data for wild-type (○) and H51Q (□) enzymes in plots A−F were determined from steady-state kinetics, and data for plots G and H were determined by stopped-flow kinetics. (A) pH dependence of V_1/E_tK_b with ethanol. Data for the wild-type enzyme are from ref *37*. (B) pH dependence of V_2/E_tK_p with acetaldehyde. Data for the wild-type enzyme are from ref *37*. (C) pH dependence of $1/K_d$ for 2,2,2-trifluoroethanol. Data for the wild-type enzyme are from ref *38*. (D) pH dependence of $1/K_d$ for *N*-cyclohexylformamide. Data for the wild-type enzyme are from ref *41*. (E) pH dependence of V_1/E_t with ethanol. Data for the wild-type enzyme are from ref *37*. (F) pH dependence of V_2/E_t with acetaldehyde. Data for the wild-type enzyme are from ref *37*. (G) pH dependence of transient oxidation of ethanol. Wild-type data are from ref *40*. (H) pH dependence of NAD^+ association. Data for the wild-type enzyme are from ref *36*. H51Q data are from ref *17*.

The kinetics for oxidation of 2-chloroethanol were also studied because the rate of hydride transfer is greatly reduced by electron withdrawal of the chloro substitution, and the pH dependence could reflect the intrinsic p*K* values. The p*K* value for V_1/E_t is shifted up by 2 pH units as compared to wild-type ADH, and the value of 7.6 might be the p*K* for the enzyme−NAD^+−alcohol complex (Table 1). The p*K* value of 9.1 for V_1/E_tK_b is somewhat higher than the value of 8.5 observed for binding of trifluorethanol, but both of these values give an estimate of p*K* values for the enzyme−NAD^+ complex (Table 1).

The pH dependencies for acetaldehyde reduction catalyzed by the H51Q enzyme were also determined with steady-state kinetics. The p*K* of 8.6 for the dependence of catalytic efficiency with acetaldehyde (V_2/E_tK_p) on pH for the wild-type enzyme is shifted to 10 for the H51Q enzyme, and the maximum value for catalytic efficiency at low pH for the protonated enzyme−NADH complex is decreased by 3-fold for the H51Q enzyme as compared to the wild-type enzyme (Figure 1B and Table 1).

The pH dependence of inhibition by *N*-cyclohexylformamide of the H51Q enzyme was best fit to a mechanism with one ionizable group where only the protonated form binds the inhibitor (Figure 1D and Table 1). The p*K* values of 10.5 (*41*) and 10.7 were observed for wild-type and H51Q enzymes, respectively. The p*K* value for *N*-cyclohexylformamide binding is a better measure of the pH dependence of the binary (E−NADH) complex than the more complex kinetic constant of V_2/E_tK_p, since binding is an equilibrium measurement. At low pH, *N*-cyclohexylformamide binds about 40-fold less well to the H51Q enzyme than to the wild-type enzyme.

The p*K* value of 7.8 for V_2/E_t for acetaldehyde reduction by the wild-type enzyme was shifted to a p*K* of 9.5 for the H51Q enzyme (Figure 2F and Table 1). The maximum turnover numbers, V_2/E_t, for wild-type and H51Q enzymes are about the same at low pH.

Kinetic Isotope Effects. Information about which steps are rate limiting in the mechanism of the H51Q enzyme was obtained by determining substrate deuterium isotope effects for ethanol oxidation with steady-state kinetics over the range of pH from 6.15 to 10.65, using a fixed concentration of 4 mM NAD^+ and varied concentrations of ethanol-d_5. The pH dependence for catalytic efficiency, V_1/E_tK_b, with ethanol-d_5 gave a p*K* value of 8.4 ± 0.1, with a limiting value at high pH of 4.7 mM^{-1} s^{-1}. The isotope effect on V_1/E_tK_b decreased from 4.5 at low pH to 2.3 at high pH, where the reaction becomes committed to catalysis. The small isotope effect indicates that hydrogen transfer is partially, but not completely, limiting for V_1/E_tK_b. The isotope effect on turnover, V_1/E_t, decreased from 2.2 at low pH to 1.2 at high pH, indicating that hydrogen transfer is partially rate limiting at low pH but not at high pH.

The kinetic constants and substrate isotope effects were also determined at pH 8 for different alcohol substrates in order to further assess the rate-limiting steps. The magnitudes of the turnover numbers, V_1/E_t, for the five different alcohols are similar (Table 2), which would be consistent with a common rate-limiting step. The isotope effects on V_1/E_t for the aliphatic alcohols indicate that hydride transfer is not rate limiting. However, the deuterium isotope effect for benzyl alcohol is 3.0, which is larger than the value of 1.4 observed for V_1/E_t with the wild-type enzyme (*26*) and comparable to the value of 3.6 observed for the transient reaction for oxidation with the wild-type enzyme (*8*). These results suggest that the relative magnitudes of rate constants controlling turnover by the H51Q enzyme have changed so that hydride transfer for benzyl alcohol (an intrinsically slower substrate) is now partially rate limiting. For the wild-type enzyme, the rate constant for hydride transfer with benzyl alcohol is 9-fold smaller than with ethanol (*40*, *43*). The observed rate constant for the transient oxidation of benzyl alcohol is 24 s^{-1} with a deuterium isotope effect of 3.6 for the wild-type enzyme (*8*), and V_1/E_t with the H51Q enzyme is 2.4 s^{-1} with an isotope effect of 3.0 (Table 2). For the H51Q enzyme, no transient burst was observed for oxidation of benzyl alcohol, suggesting that the hydride transfer step is slower than the release of NADH. It appears

Table 1: pH Dependence of Kinetic Constants for Wild-Type and H51Q Alcohol Dehydrogenases

constant	eq no.[a]	p*K*	limiting values
		Wild Type	
NAD^+ association[b]	3	6.9 ± 0.2, 9.0 ± 0.1	$k_b = 2.4\ (\pm 0.4)\ \mu M^{-1}\ s^{-1}$
$V_1/E_tK_{ethanol}$[c]	3	6.7 ± 0.1, 9.0 ± 0.1	$k_b = 22\ (\pm 1)\ mM^{-1}\ s^{-1}$
$1/K_{d,trifluoroethanol}$[d]	1	7.6 ± 0.1	$1/K_{d\ max} = 0.25\ (\pm 0.02)\ \mu M^{-1}$
$V_1/E_{t,2-chloroethanol}$[e]	1	5.5 ± 0.2	$k_a = 0.10\ (\pm 0.02)\ s^{-1}$
$k_{max,transient\ oxidation\ of\ ethanol}$[f]	1	6.4	$k_a = 155\ s^{-1}$
$V_2/E_tK_{acetaldehyde}$[c]	2	8.6 ± 0.1	$k_b = 300\ (\pm 20)\ mM^{-1}\ s^{-1}$
$1/K_{d,cyclohexylformamide}$[g]	2	10.5 ± 0.1	$1/K_{d\ max} = 0.149\ (\pm 0.005)\ \mu M^{-1}$
$V_2/E_{t,acetaldehyde}$[c]	2	7.80 ± 0.05	$k_b = 140\ (\pm 10)\ s^{-1}$
NADH association[h]	2	9.2 ± 0.2	$k_b = 11\ (\pm 1)\ \mu M^{-1}\ s^{-1}$
		H51Q	
NAD^+ association[i]	4	8.0 ± 0.2	$k_b = 3.4\ (\pm 0.9)\ mM^{-1}\ s^{-1}$ $k_a = 60\ (\pm 7)\ mM^{-1}\ s^{-1}$
$V_1/E_tK_{ethanol}$	1	8.4 ± 0.2	$k_a = 11\ (\pm 2)\ mM^{-1}\ s^{-1}$
$1/K_{d,trifluoroethanol}$[j]	1	8.5 ± 0.1	$1/K_{d\ max} = 0.24\ (\pm 0.01)\ \mu M^{-1}$
$V_1/E_{t,2-chloroethanol}$[j]	1	7.6 ± 0.1	$k_a = 0.49\ (\pm 0.01)\ s^{-1}$
$V_1/E_tK_{2-chloroethanol}$[j]	1	9.1 ± 0.2	$k_a = 3.6\ (\pm 0.5)\ mM^{-1}\ s^{-1}$
$V_1/E_{t,ethanol}$	6	7.6 ± 0.3	$k_c = 0.25\ (\pm 0.05)\ s^{-1}$
		9.3 ± 0.4	$k_b = 3\ (\pm 1)\ s^{-1}$ $k_a = 10\ (\pm 2)\ s^{-1}$
$k_{max,transient\ oxidation\ of\ ethanol}$	5	7.8 ± 0.1	$k_b = 20\ (\pm 2)\ s^{-1}$
		9.6 ± 0.1	$k_a = 93\ (\pm 6)\ s^{-1}$
$V_2/E_tK_{acetaldehyde}$	2	10.03 ± 0.05	$k_b = 102\ (\pm 5)\ mM^{-1}\ s^{-1}$
$1/K_{d,cyclohexylformamide}$	2	10.7 ± 0.1	$1/K_{d\ max} = 6.1\ (\pm 0.4)\ mM^{-1}$
$V_2/E_{t,acetaldehyde}$	2	9.5 ± 0.1	$k_b = 110\ (\pm 10)\ s^{-1}$
NADH association[i]	2	9.5 ± 0.1	$k_b = 8\ (\pm 1)\ \mu M^{-1}\ s^{-1}$

[a] The data, usually at 25 °C, were fitted to logarithmic forms of the equations given in Experimental Procedures. [b] From ref *36*. [c] From ref *37*. [d] From ref *38*. [e] From ref *39*. [f] From ref *40*. [g] From ref *41*. [h] From ref *42*. [i] From ref *17*. [j] At 30 °C.

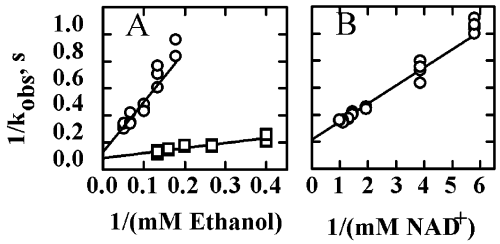

FIGURE 2: Transient reactions of the H51Q enzyme. (A) Transient oxidation of protio- (□) and deuterio- (○) ethanol. The reactions were studied with 10 μN H51Q enzyme with 2 mM NAD^+ and varied concentrations of ethanol at 25 °C at pH 8 in 33 mM sodium phosphate buffer. (B) NADH dissociation. The rate of dissociation of the enzyme−NADH complex was determined by mixing the enzyme−NADH complex (about 10 μN) with varied concentrations of NAD^+ (0.17−1.04 mM) with a fixed, saturating concentration of 15 mM pyrazole. As the NADH is displaced by NAD^+, the enzyme−NAD^+ complex is trapped by pyrazole, and the formation of the enzyme−NAD^+−pyrazole complex is followed at 294 nm. The data for k_{obs} as a function of the concentration of NAD^+ were fitted with HYPER (*21*), and the calculated maximum rate constant yields the rate constant for the dissociation of NADH (k_{off}) of 4.6 ± 0.2 s^{-1}.

that the H51Q substitution has decreased the rate constant for hydride transfer from benzyl alcohol by 10-fold.

The catalytic efficiency, V_1/E_tK_b, for the aliphatic substrates, ethanol, propanol, and butanol, increases with increasing chain length for the H51Q enzyme. These results are similar to those for wild-type ADH (*44*). A longer chain helps to position the alcohol by hydrophobic interactions for faster hydride transfer. The small isotope effects for these good substrates (propanol and butanol) indicate that hydride transfer is not rate limiting. In contrast, the isotope effect of 5.9 on V_1/E_tK_b for benzyl alcohol is larger than the value of 1.6 for the wild-type enzyme (*26*) and comparable to the value expected for an intrinsic deuterium isotope effect (*9*, *45*). Catalytic efficiency for benzyl alcohol oxidation is similar for wild-type (63 $mM^{-1}\ s^{-1}$; ref *26*) and H51Q enzymes (100 $mM^{-1}\ s^{-1}$).

Transient Kinetics and Simulation of the Overall Mechanism. The transient kinetic studies of alcohol oxidation can more directly measure hydride transfer steps. An exponential "burst" phase due to the accumulation of the complexes with NADH followed by a linear steady-state turnover is observed for the transient kinetics of ethanol oxidation when hydride transfer is faster than release of NADH. The burst reaction for the wild-type enzyme is controlled by the hydride transfer in the conversion of E−NAD^+−ethanol to E−NADH−acetaldehyde since isotope effects of 3.8−5.2 were observed (*8*, *46*).

The observed first-order rate constant for the transient oxidation of ethanol by the H51Q enzyme shows a hyperbolic dependence upon the concentration of alcohol, and the maximum rate constant is determined from the fit of the data to the HYPER equation (Figure 2A). When ethanol-d_5 was used as substrate at pH 8, the H/D isotope effect was 1.5 ± 0.2, indicating that hydride transfer is not a major rate-limiting step. Over the pH range of 6.65−10.36, the rate constant for the exponential burst phase for the H51Q enzyme increased from 1.3 to 80 s^{-1} (Figure 1G). Below a pH value of 6.65 no burst was observed, suggesting that NADH release may no longer be the rate-limiting step. The data for the H51Q enzyme were best fit to a mechanism with p*K* values of 7.8 and 9.6 with a maximum rate constant at high pH of 93 s^{-1} (Table 1). The pH dependence of the burst data resembles the pH dependence that was observed for V_1/E_t for the H51Q enzyme (Figure 1E and Table 1). In contrast, the pH dependence of hydride transfer for wild-type ADH has a p*K* value of 6.4, and the unprotonated form of the enzyme is most reactive with a maximum burst rate constant

Table 2: Substrate Deuterium Isotope Effects for H51Q Alcohol Dehydrogenase[a]

substrate	V_1/E_t (s^{-1})	$^DV_1/E_t$[b]	K_b (mM)	V_1/E_tK_b ($mM^{-1}\ s^{-1}$)	$^DV_1/E_tK_b$[b]
ethanol	1.1 ± 0.1		0.55 ± 0.05	1.9 ± 0.2	
ethanol-d_5	0.77 ± 0.06	1.4	1.3 ± 0.2	0.61 ± 0.06	3.1
propanol	1.5 ± 0.1		0.11 ± 0.01	14 ± 1	
propanol-1,1-d_2	1.4 ± 0.1	1.0	0.14 ± 0.02	11 ± 1	1.3
butanol	4.2 ± 0.3		0.045 ± 0.005	94 ± 7	
butanol-d_9	3.7 ± 0.2	1.1	0.046 ± 0.002	76 ± 4	1.2
cyclohexanol	1.15 ± 0.06		1.6 ± 0.1	0.72 ± 0.04	
cyclohexanol-d_{12}	0.56 ± 0.02	2.0	1.7 ± 0.2	0.33 ± 0.02	2.2
benzyl alcohol	2.4 ± 0.1		0.023 ± 0.001	103 ± 5	
benzyl alcohol-α,α-d_2	0.80 ± 0.06	3.0	0.046 ± 0.005	17 ± 1	5.9

[a] Initial velocities were determined at 25 °C in 33 mM sodium phosphate buffer, pH 8. A fixed concentration of about 4 mM NAD^+ was used, and the alcohol concentrations were varied. [b] Ratio of values of protio to deuterio alcohols.

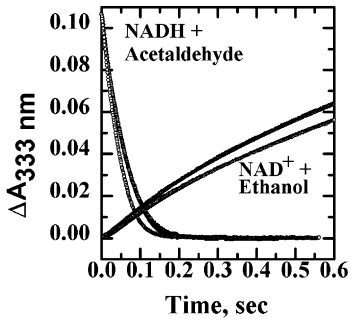

FIGURE 3: Transient data and fitted simulated curves for the oxidation of ethanol and the reduction of acetaldehyde with the H51Q enzyme. The data were fitted to the mechanism given in Scheme 3 using FITSIM. The H51Q enzyme (9.7 μN) reacted with 4.0 mM NAD^+ and 1.9 mM (◇) or 2.5 mM (△) ethanol. The H51Q enzyme (9.4 μM) reacted with 20 μM NADH and 1 mM (○) or 2 mM (□) acetaldehyde. For clarity, data are not shown for 1.88 mM ethanol and 2.0 mM acetaldehyde. The lines showing the fits are covered by the data points. The data were collected at pH 8, 25 °C.

of 155 s^{-1} (*40*). At pH 8, the rate constant for the exponential burst reaction for H51Q enzyme is decreased by 11-fold as compared to wild-type ADH.

The rate constant for the dissociation of NADH was determined for the H51Q enzyme at pH 8 (Figure 2B). For the wild-type enzyme, the release of NADH is the rate-limiting step for ethanol oxidation with a rate constant of 5.5 s^{-1} (*36*). The rate constant for dissociation of NADH from the H51Q enzyme is similar to the wild-type enzyme with a rate constant of 4.6 s^{-1}. This rate constant is close to the turnover number of about 2 s^{-1} for ethanol oxidation, suggesting that the release of NADH is also a rate-limiting step for ethanol oxidation by the H51Q enzyme.

The transient kinetics of acetaldehyde reduction were determined at pH 8 with 10 μN H51Q enzyme, 10 μM NADH, and varied concentrations of acetaldehyde. A maximum rate constant of 62 s^{-1} was determined for saturating concentrations of acetaldehyde. This value is comparable to the turnover number of 54 s^{-1} for V_2/E_t, which was determined from steady-state kinetics (*17*), and is decreased 6-fold as compared to wild-type ADH (*8*).

The effects of the H51Q substitution on the overall mechanism were defined more quantitatively by using the KINSIM/FITSIM programs to fit data from transient reactions for ethanol oxidation and acetaldehyde reduction (Figure 3). The mechanism for the simulation included the kinetically significant isomerization of the enzyme−NAD^+ complex (step 2), which was required because the rate constant for binding of NAD^+ reaches a limiting value at high concentrations of NAD^+ (*17*). The estimated rate constants for reactions of the wild-type and H51Q enzymes are compared in Table 3 for the overall mechanism given in Scheme 3.

Table 3: Estimated Rate Constants for the Mechanisms of Ethanol Oxidation and Acetaldehyde Reduction Catalyzed by Liver Alcohol Dehydrogenases[a]

rate constants	wild type[b]	H51Q[c]
k_1 ($M^{-1}\ s^{-1}$)	45×10^6	4.9×10^6
k_{-1} (s^{-1})	23000	1000
k_2 (s^{-1})	620	19
k_{-2} (s^{-1})	64	2100
k_3 ($M^{-1}\ s^{-1}$)	2.4×10^5	$1.20\ (\pm 0.02) \times 10^6$
k_{-3} (s^{-1})	560	56 ± 1
k_4 (s^{-1})	490	50 ± 10
k_{-4} (s^{-1})	610	650 ± 60
k_5 (s^{-1})	64	340 ± 80
k_{-5} ($M^{-1}\ s^{-1}$)	9.2×10^4	$1.2\ (\pm 0.1) \times 10^5$
k_6 (s^{-1})	5.5	4.6
k_{-6} ($M^{-1}\ s^{-1}$)	1.1×10^7	8.0×10^6

[a] The microscopic rate constants for the mechanism given in Scheme 3 were estimated by simulation of transient data using the KINSIM/FITSIM programs (*23*). [b] Data for the wild-type enzyme are from ref *8*. Errors were less than 10% of the values. [c] The microscopic rate constants for binding of NAD^+ and NADH to the H51Q enzyme were determined by kinetic simulations of transient data as previously described (*17*). The rate constant for dissociation of the enzyme−NADH complex was determined as shown in Figure 2B. Thus, the rate constants for NAD^+ and NADH binding (k_1, k_{-1}, k_2, k_{-2}, k_6, and k_{-6}) were fixed for these simulations. Errors for these rate constants were less than 13% of the values. Six progress curves, three forward and three reverse (Figure 3), were used in the simulation, and an *R*-squared value of 0.9988 was obtained.

Scheme 3

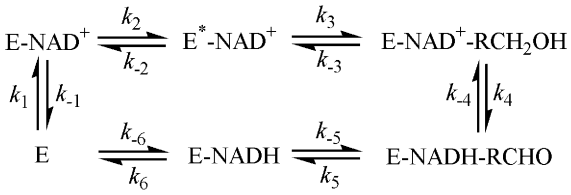

For the oxidation of ethanol, the major rate-limiting step for turnover by wild-type and H51Q enzymes appears to be the release of NADH. Significantly, the H51Q substitution decreases the rate constant, k_4, for transfer of hydrogen from the alcohol to NAD^+ by a factor of about 10. This change is not apparent in the turnover number because release of

NADH is rate limiting. The expression for the steady-state turnover number for alcohol oxidation in terms of the rate constants in Scheme 3 (*47*) is $V_1/E_t = k_2k_4k_5k_6/(k_4k_5k_6 + k_2k_4k_6 + k_2k_4k_5 + k_2k_{-4}k_6 + k_2k_5k_6)$ and is calculated from the values in Table 3 to be 3.2 s^{-1}, which is comparable to the value of 1.7 s^{-1} observed from steady-state kinetic data (*17*).

The H51Q substitution significantly affects other steps in the mechanism. The rate constants for unimolecular steps for binding of NAD^+ are changed more than 10-fold, which incidentally does not change the overall dissociation constant for NAD^+ (*17*). However, the increase in the rate constant for the isomerization, k_{-2}, from 64 to 2100 s^{-1}, and the decrease in the rate constant for release of alcohol from the E−NAD^+−alcohol complex, k_{-3}, from 560 to 56 s^{-1} for the H51Q enzyme change the rate-limiting step for acetaldehyde reduction to release of alcohol. The fitted value for k_{-3} of 56 s^{-1} compares well to the turnover number (V_2/E_t) of 54 s^{-1} for acetaldehyde reduction that was determined from steady-state kinetics and the maximum rate constant of 62 s^{-1} for the transient reduction of acetaldehyde. The expression $V_2/E_t = k_{-1}k_{-2}k_{-3}k_{-4}/(k_{-2}k_{-3}k_{-4} + k_2k_{-3}k_{-4} + k_{-1}k_{-3}k_{-4} + k_{-1}k_{-2}k_{-4} + k_{-1}k_{-2}k_4 + k_{-1}k_{-2}k_{-3})$ reduces to k_{-3} since k_{-2} is large relative to k_2, k_{-4} is large relative to k_4, and the other rate constants are large relative to k_{-3}, the microscopic rate constant for alcohol release.

X-ray Crystallography. Structures were determined for the doubly substituted Q51R228 ADH complexed with NAD^+ and 2,4-difluorobenzyl alcohol or 2,3-difluorobenzyl alcohol in order to demonstrate that Gln could substitute for His-51 and maintain hydrogen-bonding interactions with the coenzyme. Moreover, it is of interest to determine how Arg-228 can replace Lys in the structure because we used the Q51R228 enzyme for the studies on the pH dependence of coenzyme binding (*17*) and because the Lys is substituted with Arg in many of the homologous dimeric plant ADHs (*14*). The K228R substitution has moderate effects on coenzyme binding (*17*). The difluorobenzyl alcohols are unreactive as substrates but sterically similar to benzyl alcohol and thus potentially good analogues of the Michaelis complex of the enzyme, as we found for 2,3,4,5,6-pentafluorobenzyl alcohol (*6*). Thus, the structures can show how the enzyme recognizes differently substituted benzyl alcohols, increasing our knowledge of enzyme specificity.

Although the crystals were small, the X-ray data are very good to 1.8 Å. The refinements provide excellent structures, with good statistics (Table 4), and all amino acid residues except cysteines 174 (Zn ligands at the active site) are in allowed regions of the Ramachandran plot. One dimeric molecule is found in the asymmetric unit, but the two subunits have very similar structures, with an rmsd of 0.13 Å for superpositioning of subunits A and B of the Q51R228 enyzme complexed with 2,4-difluorobenzyl alcohol and 0.08 Å for the subunits of the enzyme with 2,3-difluorobenzyl alcohol. Both structures have the "closed" conformation as is usually found for ternary complexes of ADH (*48*). The subunits of the Q51R228 enzyme complexed with 2,4-difluorobenzyl alcohol superimpose onto the subunits of the wild-type enzyme complexed with 2,3-difluorobenzyl alcohol (1MG0.pdb) with an rmsd of 0.24 Å (average for eight subunits since the wild-type enzyme has four subunits in the asymmetric unit) or the wild-type enzyme complexed with 4-iodopyrazole (1N92.pdb) with an rmsd of 0.21 Å. Thus the overall conformation of the Q51R228 enzyme is very similar to the structures of ternary complexes of the wild-type enzyme.

Table 4: X-ray Data and Refinement Statistics for Q51R228 Horse Liver Alcohol Dehydrogenase Complexed with NAD^+ and Difluorobenzyl Alcohols

difluorobenzyl alcohol	2,4-	2,3-
space group	*P*1	*P*1
PDB entry	1QV6	1QV7
dimeric molecules per unit cell	1	1
cell dimensions (Å)	44.3, 51.1, 92.7	44.1, 51.0, 92.5
cell angles (deg)	91.6, 103.1, 109.9	91.6, 103.0, 109.9
resolution range (Å)	10−1.8	20−1.8
measured reflections: total, unique	124354, 63963	132501, 67918
completeness (%) (outer shell)	93.3 (93.6)	95.1 (94.5)
R_{sym} (%) (outer shell)[a]	6.3 (22)	11 (39)
mean $\langle I\rangle/\sigma\langle I\rangle$ (outer shell)	7.5 (3.3)	7.3 (2.5)
R_{value}, R_{free}, test %[b]	15.7, 20.3, 2.5	17.8, 22.2, 2.5
rmsd for bond distances (Å)[c]	0.020	0.020
rmsd for bond angles (deg)[c]	1.8	1.8
water molecules per unit cell	579	489

[a] $R_{sym} = (\sum|I - \langle I\rangle|)/\sum\langle I\rangle$, where I is the integrated intensity of a given reflection. [b] $R_{value} = (\sum|F_o - kF_c|)/\sum|F_o|$, where k is a scale factor. The R_{free} value was calculated with the indicated percentage of reflections not used in the refinement. [c] Root-mean-square deviations (rmsd) from ideal geometry in the final models.

Figure 4 shows that the positions of the difluorobenzyl alcohols in the two different complexes are well-defined in electron density maps. The difluorobenzyl alcohols bind in similar positions, with the fluorine atoms oriented away from the nicotinamide ring and interacting hydrophobically with amino acid side chains. Likewise, Figure 5 shows that the positions for the Gln-51 residue are well-defined, although the carboxamido groups have somewhat higher temperature factors than the peptide backbone atoms.

As shown in Figure 6A, Gln-51 can readily participate in the hydrogen bond network that connects the alcohol bound to the catalytic zinc, as the carbonyl oxygen of the carboxamido group is in position to hydrogen bond to the 2′-hydroxyl group of the nicotinamide ribose, at a distance of 2.5 Å. Although the electron density clearly defines the position of Gln-51, it cannot unambiguously define whether the carbonyl oxygen or the amido nitrogen of the carboxamido group forms the hydrogen bond to the ribose. In the refined structure of the complex with 2,4-difluorobenzyl alcohol, the amido nitrogen is 3.2 Å from the carbonyl oxygen of Val-294 and thus may form a hydrogen bond (Table 5). The amido nitrogen is 3.3 Å from the 3′-hydroxyl group of the ribose, which is a hydrogen bond donor to the carbonyl oxygen of Ile-269. Furthermore, the water molecule that is hydrogen bonded to the carbonyl oxygens of Val-294 and Gly-270 also must be an acceptor of a hydrogen bond from the amido group of Gln-51. Thus, the best interpretation, based on consideration of the hydrogen bonds, is that the carboxamido oxygen of Gln-51 makes a hydrogen bond with the 2′-hydroxyl group of the ribose, which would require that the alcohol bound to zinc retains its proton in the complex.

However, the temperature factors for the atoms in the carboxamido group are somewhat higher than for atoms in

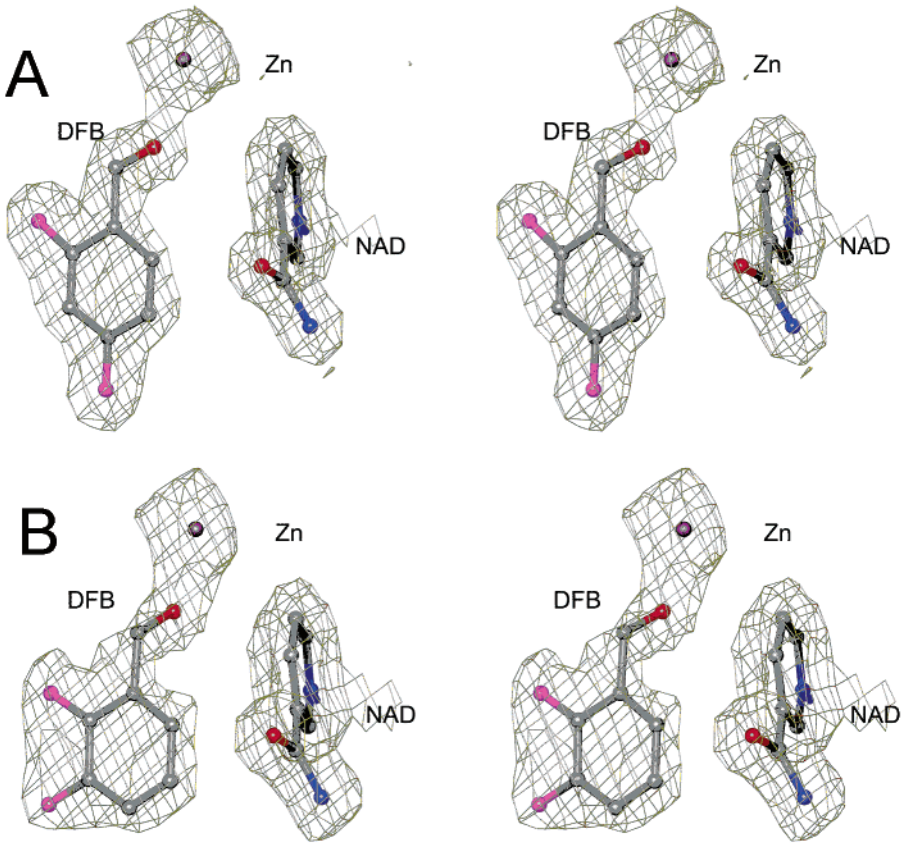

FIGURE 4: Electron density maps defining the positions of the difluorobenzyl alcohols in the Q51R228 enzyme−NAD^+ complexes. (A) Complex with 2,4-difluorobenzyl alcohol. (B) Complex with 2,3-difluorobenzyl alcohol.

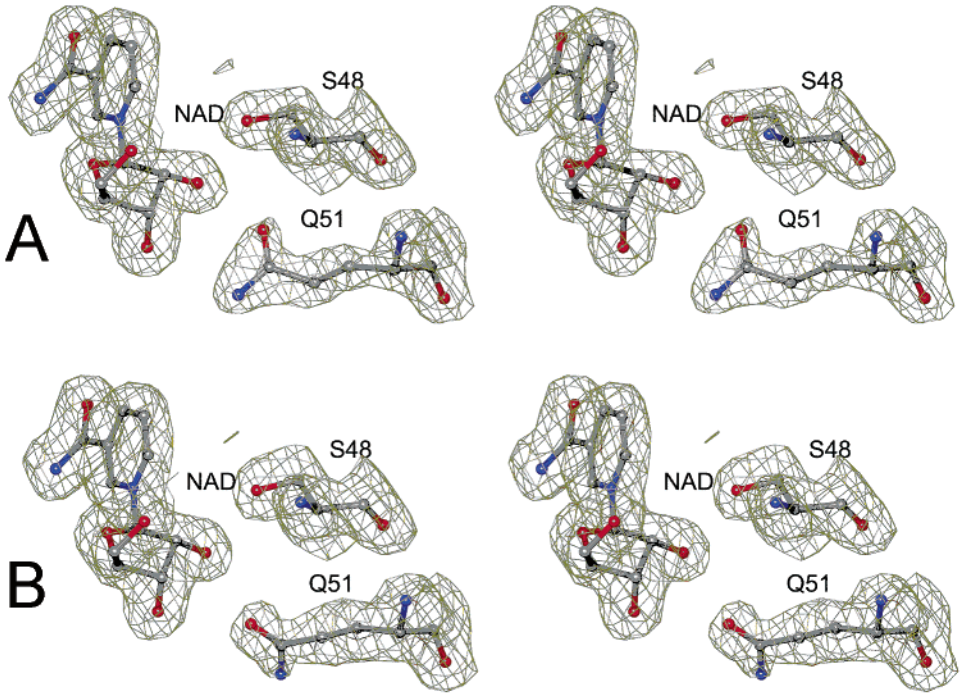

FIGURE 5: Electron density maps defining the positions of Gln-51 in complexes with the Q51R228 enzyme. (A) Complex with 2,4-difluorobenzyl alcohol. (B) Complex with 2,3-difluorobenzyl alcohol.

the peptide backbone, and we suggest that the carboxamide could rotate so that the amido group donates a hydrogen to the 2′-hydroxyl group. This might occur when an aldehyde or formamide binds to the enzyme−NADH complex. In any case, Gln-51 fits well into the structure and apparently stabilizes the binding of the coenzyme as well as His-51 does since the affinity for the coenzyme is not altered by the H51Q substitution. Although the glutamine cannot act as an acid or base catalyst, and it would block access of solvent water to the ribose in the observed position, there is sufficient space for the side chain of the Gln-51 to rotate away from the ribose and allow access of solvent.

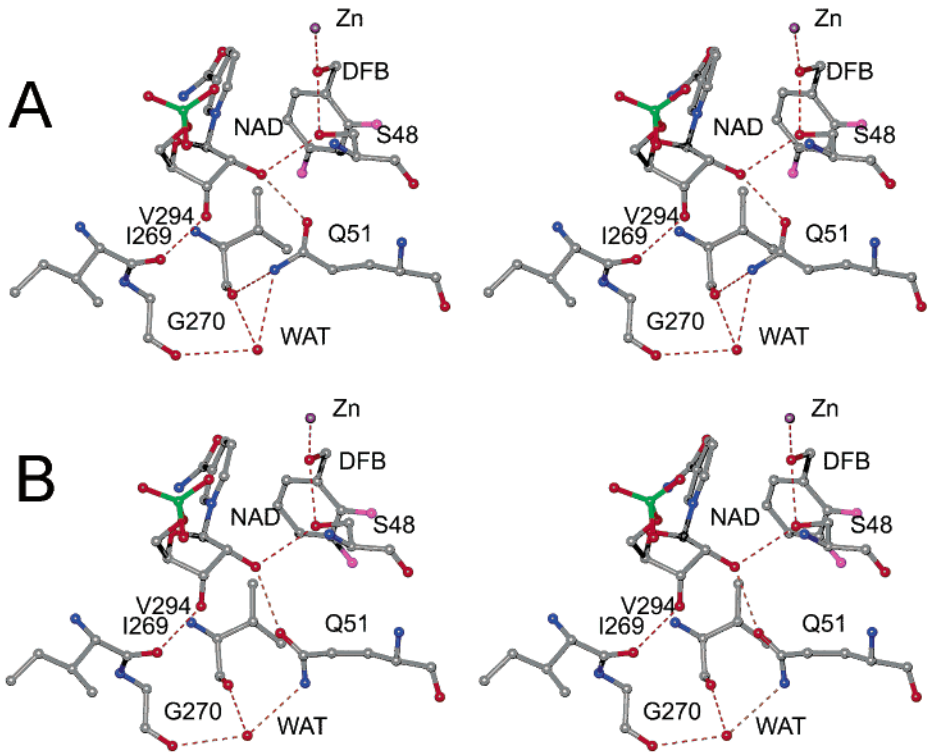

FIGURE 6: Structures of the Q51R228 enzyme complexed with NAD^+ and difluorobenzyl alcohols. Hydrogen bonds (dashed red lines) are inferred from the close contacts (2.6−3.2 Å). (A) Complex with 2,4-difluorobenzyl alcohol. (B) Complex with 2,3-difluorobenzyl alcohol.

Table 5: Distances in the Active Sites of Liver Alcohol Dehydrogenases Complexed with Difluorobenzyl Alcohols[a]

enzyme	wild type[b]	Q51R228	Q51R228
difluorobenzyl alcohol	2,3-	2,3-	2,4-
resolution (Å)	1.8	1.8	1.8
distance between atoms (Å)			
Zn−S C46	2.33	2.34	2.27
Zn−S C176	2.27	2.18	2.20
Zn−NE2 H67	2.10	2.08	2.18
Zn−O ALC378[c]	2.11	2.22	2.23
OG S48−O ALC378	2.63	2.71	2.68
OG S48−O2′N NAD	2.64	2.90	2.89
NE2 H51−O2′N NAD	3.03		
NE2 H51−O3′N NAD	3.09		
O I269−O3′N NAD	2.70	2.92	2.91
OE1 Q51−O2′N NAD		2.71	2.53
NE2 Q51−O3′N NAD		4.82	3.32
NE2 Q51−O V294		3.28	3.15
C4N NAD−C7 ALC378	3.66, 3.86	3.91	4.06

[a] For the wild-type enzyme, the numbers represent averages for the four independent subunits in the asymmetric unit (*49*), and for the Q51R228 enzyme, the numbers are averages for the two independent subunits. [b] PDB entry 1MG0 (*49*). [c] ALC378 is the bound alcohol.

The orientation of the side chain of Gln-51 in the complex of the Q51R228 enzyme with NAD^+ and 2,3-difluorobenzyl alcohol (Figure 6B) is somewhat different than in the complex with 2,4-difluorobenzyl alcohol (Figure 6A). The carboxamido oxygen may form a hydrogen bond with the 2′-hydroxyl of the ribose, as the distance is about 2.7 Å, but the amido nitrogen is 4.8 Å from the 3′-hydroxyl group due to a rotation of the carboxamido group. The amido nitrogen is 3.3 Å from the carbonyl oxygen of Val-294, but it makes a hydrogen bond to the water that is hydrogen bonded to the carbonyl oxygens of Gly-270 and Val-294. It is not obvious from the structures why the interactions of Gln-51 in the two different complexes are somewhat different, but the similar interactions could produce the same effects with respect to coenzyme binding and the proton relay system.

The difluorobenzyl alcohols bind in a position (Figures 4 and 6) that is shifted slightly from the position found for 2,3,4,5,6-pentafluorobenzyl alcohol in the complex with the wild-type enzyme and NAD^+ but very similar to the position found with *p*-bromobenzyl alcohol or one of the conformations for 2,3-difluorobenzyl alcohol (*6*, *49*). The methylene carbons (C7) of the difluorobenzyl alcohols in the complexes with Q51R228 ADH are about 4.0 Å from C4 of the nicotinamide ring, with the *pro-R* hydrogen of the alcohol pointing away from the nicotinamide ring, whereas in the wild-type enzyme with pentafluorobenzyl alcohol, the distance is about 3.4 Å, with the *pro-R* hydrogen pointing toward C4 of the nicotinamide ring (1HLD.pdb; ref *6*). Rotations about the single bonds in the difluorobenzyl alcohols can lead to a small shift in the benzene ring so that C7 is in the position observed for the pentafluorobenzyl alcohol where hydrogen transfer to C4 of the nicotinamide ring would appear to be most direct. The 2,3-difluorobenzyl alcohol binds to the wild-type enzyme in two conformations, where the benzene ring is flipped about 180° and shifted slightly, indicating that there is substrate mobility (*49*). However, only one major conformation is observed for the difluorobenzyl alcohols in the complexes with the Q51R228 enzyme. In these complexes, the two fluorines interact with hydrophobic side chains of Val-57, Leu-116, Phe-140, Leu-141, and Val-294, but such interactions are weak and only one factor in binding (*50*). The difference in conformational preference of wild-type and H51Q ADHs for the 2,3-difluorobenzyl alcohols may also be related to the small differences in the distances between the oxygen of the alcohol and the zinc or hydroxyl group of Ser-48 (Table 5).

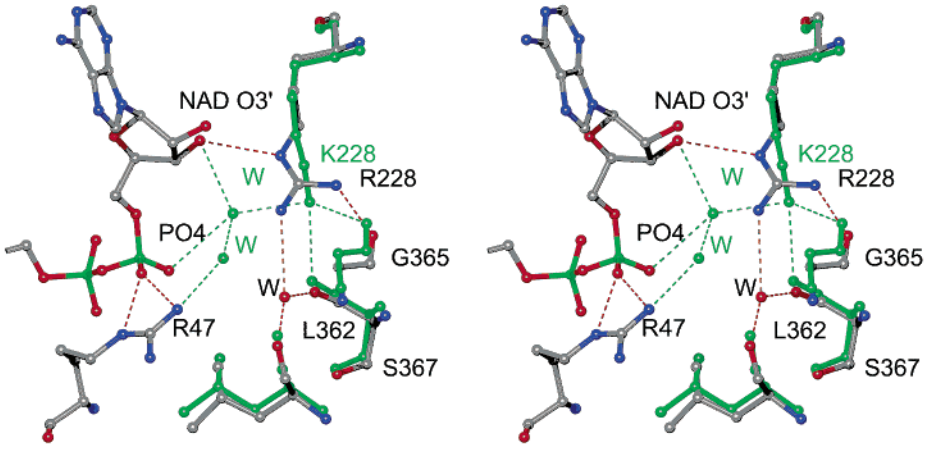

FIGURE 7: Positions of Arg-228 in the Q51R228 enzyme and of Lys-228 in the wild-type enzyme. The coenzyme binding domains of the structures were superimposed. The gray and color-coded model is the Q51R228 enzyme (1QV6.pdb), and the green model represents the wild-type enzyme complexed with NAD^+ and 2,3-difluorobenzyl alcohol, determined at 1.8 Å (1MG0.pdb). There is a small shift of Ser-367 and Leu-362 in the Q51R228 enzyme as compared to the wild-type enzyme, but the α carbons of the subunits superimpose with an rmsd of 0.22 Å.

If the protonated benzyl alcohols bind to the Q51R228 enzyme, that is, with the hydroxyl group of the alcohol donating a hydrogen to the nearby hydroxyl group of Ser-51, the distances between the alcohol oxygen and its neighbors should be longer than if the alkoxides were present. We expect that an alkoxide would interact more strongly, with shorter distances, with the positively charged zinc and hydrogen-bonded partners than would a protonated alcohol. Benzyl alcohol probably binds as the alkoxide at pH 7 in wild-type ADH, as this would explain the apparent p*K* value of 6.4 for the dependence of the hydride transfer rate on pH (*43*) and the inverse solvent isotope effect due to a low-barrier hydrogen bond (*8*, *9*). Calculations suggest that the alkoxide more readily transfers the hydride ion than the protonated alcohol and that the zinc−oxygen distance increases from about 1.95 Å for the alkoxide to 2.15 Å for the product aldehyde (*10*, *51*). The distance observed between the catalytic zinc and the oxygen of 2,3-difluorobenzyl alcohol is 2.2 Å for the complex with the H51Q enzyme, as compared to 2.1 Å for the wild-type enzyme, and the distance between the alcohol oxygen and the serine hydroxyl is 2.7 Å for the H51Q enzyme, as compared to 2.6 Å for the wild-type enzyme (Table 5). The slightly longer distances for H51Q ADH are more consistent with a bound alcohol rather than an alkoxide.

As shown in Figure 7, the arginine side chain in the complex of the Q51R228 enzyme with NAD^+ and 2,4-difluorobenzyl alcohol is readily accommodated in the coenzyme binding site, with only a small shift of the peptide backbone of the catalytic domain as compared to the wild-type enzyme. The position of Lys-228 represents the predominant conformation in the wild-type enzyme; a water molecule bridges between the ϵ-amino group and the adenosine phosphate. In the Q51R228 enzyme, two water molecules are displaced by the guanidino group, which makes a hydrogen bond to the 3′-hydroxyl group of the adenosine and interacts with the adenosine phosphate. Although Arg-228 fits well into the AMP binding site, small steric and electrostatic effects decrease affinities for coenzymes by 3−7-fold (*17*).

DISCUSSION

His-51 appears to have a significant role in catalysis by horse liver alcohol dehydrogenase, as suggested from studies of three-dimensional structures of the enzyme and its complexes, pH dependencies of the kinetics of catalysis, and chemical modification. The contribution of His-51 to catalysis was evaluated by using site-directed mutagenesis to substitute the ionizable imidazole group with the neutral carboxamido group of glutamine and by examining the kinetics of various steps of the mechanism. Previous work showed that the pH dependence for NAD^+ binding was significantly altered by the H51Q substitution, and we concluded that His-51 would facilitate the ionization of the water ligated to the catalytic zinc and the isomerization of the enzyme−NAD^+ complex that controls binding (*17*). The present results show that the H51Q substitution significantly changes the pH dependencies and rate constants for binding and reaction of alcohols, further supporting a role for His-51 in base catalysis. The results will be discussed in terms of the enzyme species that are involved in the various kinetic parameters.

The pH dependencies for catalytic efficiency, V_1/E_tK_b, on ethanol and the binding of 2,2,2-trifluoroethanol are shifted from a p*K* of about 7.2 for wild-type ADH to about 8.5 for H51Q ADH (Figure 1 and Table 1). The p*K* value for wild-type ADH was also found for the pH dependences of V_1/E_tK_b for cyclohexanol and $1/K_d$ for 2,2,2-trifluoroethanol in another study (*52*). For the simple ordered bi-bi mechanism, this p*K* value arises from the enzyme−NAD^+ complex and is most reasonably interpreted as being due to the water ligated to the catalytic zinc (*1*). The water is displaced by the hydroxyl group of the alcohols, as shown by X-ray crystallography (*2*, *6*, *53*). His-51 could facilitate deprotonation of the zinc−water through the proton relay system and lead to more favorable binding, whereas Gln-51 would not. The pH dependence is not abolished by the H51Q substitution because the zinc−water is still present, and thus we suggest that His-51 modulates the ionization of the zinc ligand. The H51Q substitution decreases the catalytic efficiency for oxidation of ethanol at pH 7 by 35-fold, but

only 2-fold at high pH where the zinc−water can ionize without assistance by His-51.

The reaction of 2-chloroethanol also gives useful information about the p*K* values of the enzyme complexes. For the oxidation of 2-chloroethanol, hydride transfer is apparently rate limiting because the turnover numbers for 2-chloroethanol are 50- and 9-fold smaller than the rate constants for dissociation of NADH from the wild-type and H51Q enzymes, respectively (Table 1). The electron-withdrawing chloride significantly decreases the rate of hydride transfer. The p*K* value of 9.1 for the catalytic efficiency, V_1/E_tK_b, indicates that the p*K* for the H51Q enzyme−NAD^+ complex has shifted from the value of 7.2 for the wild-type enzyme. The pH dependence for the turnover numbers for the oxidation of 2-chloroethanol shows that the p*K* of the enzyme−NAD^+−alcohol complex is shifted up from 5.5 for wild-type ADH to 7.5 for H51Q ADH (Table 1).

The p*K* values of free water, ethanol, 2-chloroethanol, and 2,2,2-trifluoroethanol of 15.4, 15.9, 14.3, and 12.4, respectively, are decreased in the ternary complexes with the wild-type enzyme and NAD^+ to 7.6, 6.4, 5.5, and 4.3 (*39*). The systematic depression of p*K* values is probably due to ligation of the alcohol to the catalytic zinc adjacent to the positive charge of the nicotinamide ring. From the analysis of the H51Q enzyme, the p*K* values for water and 2-chloroethanol in the ternary complex are increased by 1−2 units, to 8.5−9.1 and 7.6, respectively. These results suggest that His-51 contributes to the ionization of the alcohol through the proton relay system.

The pH dependencies for the turnover number, V_1/E_t, and the observed rate constant for the transient oxidation of ethanol for H51Q ADH are similar (Figure 1E,G) but complex because isomerization of the enzyme−NAD^+ complex (k_2), release of NADH (k_6), and hydride transfer (k_4) are each partially rate limiting. As discussed previously, NAD^+ association to ADH is a two-step process that includes a bimolecular binding step and an isomerization that could be due to a conformational change (*17*). The apparent rate constant for association of NAD^+ is given by the equation $k_1k_2/(k_{-1} + k_2)$, for the mechanism in Scheme 3, but since k_2 is small relative to k_{-1} for H51Q ADH at pH 8, the equation simplifies to k_1k_2/k_{-1}. Because the pH dependence for NAD^+ binding to the H51Q enzyme (Figure 1H) is similar to that for the Q51R228 enzyme (*17*), where the association rate constant is controlled by k_2 over the observed pH range, the p*K* value of 8.0 that is observed for NAD^+ association to H51Q ADH is most likely due to the isomerization step, k_2. The observed pH dependence is probably due to the ionization of the catalytic zinc−water, where the zinc hydroxide electrostatically attracts the positive charge of the nicotinamide ring and properly positions the NAD^+ for the conformational change.

The pH dependence for the transient oxidation of ethanol by the H51Q enzyme is described by p*K* values of 7.8 and 9.6 (Table 1 and Figure 1G). The complexity suggests that there are differential changes in rate-limiting steps as a function of pH. The small substrate isotope effect of 1.5 for the exponential burst reaction at pH 8 suggests that the hydride transfer is only partially rate limiting. In the low pH region, the p*K* value of 7.8 may be controlled by the isomerization of the E−NAD^+ complex. At higher pH, the p*K* value of 9.6 may correspond to the deprotonation of the enzyme−NAD^+−alcohol complex. The H51Q substitution has significantly decreased the rate constant for the transient reaction and has altered the pH dependence from that observed for wild-type ADH (Figure 1G; ref *40*).

The p*K* value of 9.5 for the turnover of acetaldehyde (V_2/E_t) supports the conclusion that the H51Q enzyme−NAD^+−alcohol complex has a p*K* of 9.6. Release of alcohol is the rate-limiting step for the turnover of acetaldehyde at pH 8 as determined from the simulation of the overall mechanism (Scheme 3 and Table 3). On the assumption that the release of alcohol is rate limiting over the observed pH range, the p*K* value of 9.5 may be assigned to the protonation of the enzyme−NAD^+−alcoholate complex prior to the release of alcohol. The protonated form of the alcohol (R−OH) should be released faster than the alkoxide form (RO^-), as the alkoxide should be stabilized by its interaction with the catalytic zinc ion and the positive charge of the nicotinamide ring of NAD^+. The p*K* value of 9.5 for the H51Q enzyme is shifted up as compared to the p*K* values of 6.6−7.2 that are observed for the release of alcohols from the enzyme−NAD^+−alcohol complex in the wild-type enzyme (*8*, *54*, *55*). In the wild-type enzyme, the p*K* value is lower because His-51 can donate a proton to the alkoxide through the proton relay system. It is important to note that the transient rate of reaction of the wild-type enzyme−NADH−aldehyde complex, that is, the hydride transfer step, is pH independent over the range of pH 6.0−9.9 with aromatic aldehydes (*43*, *56*). Thus, the state of protonation of His-51 does not appear to affect the reduction of aldehydes over this pH range, and the H51Q substitution should not affect this step.

The ionization of the binary enzyme−NADH complex was analyzed by studying the pH dependence of the binding of *N*-cyclohexylformamide. The p*K* value of 10.7 for the H51Q enzyme is close to the value of 10.5 that is observed for wild-type ADH (*41*). For the wild-type enzyme, p*K* values of 10 and 11.2 have also been observed for isobutyramide (*52*) and 4-*trans*-(*N*,*N*-dimethylamino)cinnamaldehyde (*57*), which are inhibitors that bind to the E−NADH complex. Ionization of the catalytic zinc water may account for the p*K* value, which is shifted about 2 units higher in the enzyme−NADH complex than in the enzyme−NAD^+ complex. The positive charge on the oxidized nicotinamide ring should depress the p*K* value of the water as compared to the neutral, reduced nicotinamide ring. Binding of *N*-cyclohexylformamide is tightest at low pH because the inhibitor can more readily displace a water as compared to the hydroxide. Although the p*K* value is not affected by the H51Q substitution, the affinity is decreased by 40-fold. This may result from altered hydrogen-bonding interactions in the ternary complex, where the amido group of Gln-51 would donate a hydrogen bond to the 2′-hydroxyl of the NADH and the carbonyl group of the inhibitor would accept a hydrogen bond from Ser-48 in order to form the complete network of hydrogen bonds. As compared to the network illustrated in Figure 6, the carboxamido group of Gln-51 would be rotated 180° and the water might be displaced.

As presented previously, the pH dependence of NADH association provided a p*K* value of 9.5 for the free H51Q enzyme, a value very similar to the p*K* value of 9.2 for the wild-type enzyme (*17*). Thus His-51 does not control the pH dependence for NADH association to the free enzyme.

Site-directed mutagenesis is a useful tool for studying the participation of an amino acid residue in catalysis, but any substitution can alter the structure of the enzyme and affect activity by steric in addition to chemical effects (*13*). Structural effects are difficult to exclude. Nevertheless, X-ray crystallography shows that the structure of the enzyme with the H51Q substitution is very similar to the structures of the complexes with the wild-type enzyme and that the glutamine residue can make a hydrogen bond to the coenzyme in place of the histidine (Figure 6). This good interaction can explain why the overall affinities for NAD^+ or NADH are not affected by the H51Q substitution. Therefore, we conclude that gross structural alterations are not responsible for the changes in kinetics of H51Q ADH. Since the crystalline Q51R228 enzyme is isomorphous with ternary complexes of the wild-type enzyme, with similar unit cell dimensions in the *P*1 space group, and the overall conformation of the doubly substituted enzyme is the same as the wild-type enzyme, it is likely that the H51Q enzyme has a very similar structure.

As enzymologists try to determine the basis for catalytic activity of enzymes, the evaluation of the contribution of histidine residues by site-directed mutagenesis has led to various results. Substitutions with Ala or Gln can decrease activity by $10-10^6$-fold, and some investigators suggest that the residual activity indicates that the His does not function as a base catalyst as proposed from structural and other studies (*58*, *59*). However, in those cases where the His is exposed to the solvent and X-ray crystallography shows that the substitution does not significantly alter the structure, the changes in activity may be an estimate of the contribution to catalysis (*13*). For instance, the 20-fold decrease in activity of carbonic anhydrase II as a result of the substitution of His-64 with Ala was interpreted as support for a role of the His in a proton shuttle (*60*). Clearly, interpretations require comprehensive studies of the wild-type and mutated enzymes to evaluate effects on structure, mechanism, pH dependencies, and kinetics. For instance, the substitution of Pro-47 with His in mouse ADH2 increases catalytic efficiency for alcohol oxidation by about 100-fold, but the Pro47Ala substitution does likewise, and pH dependence studies suggest that His-47 does not provide base catalysis (*61*, *62*). Eventually, we may find consensus in evaluating the quantitative contribution of His residues.

Although the steady-state kinetic constants of ADH at pH 8 are not dramatically affected by the H51Q substitution, detailed analysis of coenzyme binding, transient kinetics, and pH dependencies shows significant effects on catalysis. In particular, the reactions of the H51Q enzyme with NAD^+ and alcohol have decreased rate constants and increased p*K* values compared to wild-type ADH. It appears that His-51 contributes to catalysis by acting as a base to facilitate removal of a proton from the water or alcohol bound to the catalytic zinc through the proton relay system and as an acid for aldehyde reduction by donating a proton to the alkoxide. His-51 participates in catalysis, but it is not the only group that contributes to rate enhancement and pH dependencies. His-51 is not essential for catalysis but rather modulates activity.

ACKNOWLEDGMENT

We thank the ESRF, Grenoble, France, for support of travel and the collection of synchrotron data, the Strategic Research Foundation of Sweden for support of travel, and Yngve Cerenius for assistance with data collection at the MAXLAB in Lund, Sweden. Dr. Ramaswamy also acknowledges support from the Department of Molecular Biology and Hans Eklund, Swedish University of Agricultural Sciences, Uppsala, Sweden, for part of the work.

REFERENCES

1. Brändén, C.-I., Jörnvall, H., Eklund, H., and Furugren, B. (1975) Alcohol Dehydrogenases, *The Enzymes, 3rd Ed. 11*, 103−190.
2. Eklund, H., Plapp, B. V., Samama, J. P., and Brändén, C.-I. (1982) Binding of substrate in a ternary complex of horse liver alcohol dehydrogenase, *J. Biol. Chem. 257*, 14349−14358.
3. Hennecke, M., and Plapp, B. V. (1983) Involvement of histidine residues in the activity of horse liver alcohol dehydrogenase, *Biochemistry 22*, 3721−3728.
4. Plapp, B. V., Ganzhorn, A. J., Gould, R. M., Green, D. W., Jacobi, T., Warth, E., and Kratzer, D. A. (1991) Catalysis by yeast alcohol dehydrogenase, *Adv. Exp. Med. Biol. 284*, 241−251.
5. Ehrig, T., Hurley, T. D., Edenberg, H. J., and Bosron, W. F. (1991) General base catalysis in a glutamine for histidine mutant at position 51 of human liver alcohol dehydrogenase, *Biochemistry 30*, 1062−1068.
6. Ramaswamy, S., Eklund, H., and Plapp, B. V. (1994) Structures of horse liver alcohol dehydrogenase complexed with NAD^+ and substituted benzyl alcohols, *Biochemistry 33*, 5230−5237.
7. Niederhut, M. S., Gibbons, B. J., Perez-Miller, S., and Hurley, T. D. (2001) Three-dimensional structures of the three human class I alcohol dehydrogenases, *Protein Sci. 10*, 697−706.
8. Sekhar, V. C., and Plapp, B. V. (1990) Rate constants for a mechanism including intermediates in the interconversion of ternary complexes by horse liver alcohol dehydrogenase, *Biochemistry 29*, 4289−4295.
9. Ramaswamy, S., Park, D. H., and Plapp, B. V. (1999) Substitutions in a flexible loop of horse liver alcohol dehydrogenase hinder the conformational change and unmask hydrogen transfer, *Biochemistry 38*, 13951−13959.
10. Agarwal, P. K., Webb, S. P., and Hammes-Schiffer, S. (2000) Computational studies of the mechanism for proton and hydride transfer in liver alcohol dehydrogenase, *J. Am. Chem. Soc. 122*, 4803−4812.
11. Cui, Q., Elstner, M., and Karplus, M. (2002) A theoretical analysis of the proton and hydride transfer in liver alcohol dehydrogenase (LADH), *J. Phys. Chem. B 106*, 2721−2740.
12. Dickenson, C. J., and Dickinson, F. M. (1977) A study of the ionic properties of the essential histidine residue of yeast alcohol dehydrogenase in complexes of the enzyme with its coenzymes and substrates, *Biochem. J. 161*, 73−82.
13. Plapp, B. V. (1995) Site-directed mutagenesis: a tool for studying enzyme catalysis, *Methods Enzymol. 249*, 91−119.
14. Sun, H. W., and Plapp, B. V. (1992) Progressive sequence alignment and molecular evolution of the zn-containing alcohol dehydrogenase family, *J. Mol. Evol. 34*, 522−535.
15. Ramaswamy, S., el Ahmad, M., Danielsson, O., Jörnvall, H., and Eklund, H. (1996) Crystal structure of cod liver class I alcohol dehydrogenase: Substrate pocket and structurally variable segments, *Protein Sci. 5*, 663−671.
16. Davis, G. J., Carr, L. G., Hurley, T. D., Li, T.-K., and Bosron, W. F. (1994) Comparative roles of histidine 51 in human $\beta1\beta1$ and threonine 51 in $\pi\pi$ alcohol dehydrogenases, *Arch. Biochem. Biophys. 311*, 307−312.
17. LeBrun, L. A., and Plapp, B. V. (1999) Control of coenzyme binding to horse liver alcohol dehydrogenase, *Biochemistry 38*, 12387−12393.
18. Park, D. H., and Plapp, B. V. (1991) Isoenzymes of horse liver alcohol dehydrogenase active on ethanol and steroids. cDNA cloning, expression, and comparison of active sites, *J. Biol. Chem. 266*, 13296−13302.
19. Theorell, H., and Yonetani, T. (1963) Liver alcohol dehydrogenase-DPN-pyrazole complex: A model of a ternary intermediate in the enzyme reaction, *Biochem. Z. 338*, 537−553.

20. Jörnvall, H. (1970) Horse liver alcohol dehydrogenase. The primary structure of an N-terminal part of the protein chain of the ethanol-active enzyme, *Eur. J. Biochem. 14*, 521−534.
21. Cleland, W. W. (1979) Statistical analysis of enzyme kinetic data, *Methods Enzymol. 63*, 103−138.
22. Andersson, P., and Pettersson, G. (1982) Kinetic equivalence of the subunits of liver alcohol dehydrogenase, *Eur. J. Biochem. 122*, 559−568.
23. Frieden, C. (1994) Analysis of kinetic data: practical applications of computer simulation and fitting programs, *Methods Enzymol. 240*, 311−322.
24. Gould, R. M., and Plapp, B. V. (1990) Substitution of arginine for histidine-47 in the coenzyme binding site of yeast alcohol dehydrogenase I, *Biochemistry 29*, 5463−5468.
25. Johnson, M. L., and Frasier, S. G. (1985) Nonlinear least-squares analysis, *Methods Enzymol. 117*, 301−342.
26. Dworschack, R. T., and Plapp, B. V. (1977) pH, isotope, and substituent effects on the interconversion of aromatic substrates catalyzed by hydroxybutyrimidylated liver alcohol dehydrogenase, *Biochemistry 16*, 2716−2725.
27. Leslie, A. G. W. (1992) *Joint CCP4 and ESF-EACMB Newsletters on Protein Crystallography*, No. 26, Daresbury Laboratory, Warrington, U.K.
28. Collaborative Computational Project, Number 4 (1994) The CCP4 Suite: Programs for Protein Crystallography, *Acta Crystallogr. D50*, 760−763.
29. Kabsch, W. (1993) Automatic processing of rotation diffraction data from crystals of initially unknown symmetry and cell constants, *J. Appl. Crystallogr. 26*, 795−800.
30. Navaza, J. (1994) AMoRe: an automated package for molecular replacement, *Acta Crystallogr. A50*, 157−163.
31. Jones, T. A., Zou, J. Y., Cowan, S. W., and Kjeldgaard (1991) Improved methods for building protein models in electron density maps and the location of errors in these models, *Acta Crystallogr. A47*, 110−119.
32. Perrakis, A., Sixma, T. K., Wilson, K. S., and Lamzin, V. S. (1997) wARP: Improvement and extension of crystallographic phases by weighted averaging of multiple-refined dummy atomic models, *Acta Crystallogr. D53*, 448−455.
33. Laskowski, R. A., MacArthur, M. W., Moss, D. S., and Thornton, J. M. (1993) PROCHECK: a program to check the stereochemical quality of protein structures, *J. Appl. Crystallogr. 26*, 286−290.
34. Harris, M., and Jones, T. A. (2001) MOLRAY−a web interface between O and the POV−Ray ray tracer, *Acta Crystallogr. D57*, 1201−1203.
35. Cleland, W. W. (1977) Determining the chemical mechanisms of enzyme-catalyzed reactions by kinetic studies, *Adv. Enzymol. 45*, 273−387.
36. Sekhar, V. C., and Plapp, B. V. (1988) Mechanism of binding of horse liver alcohol dehydrogenase and nicotinamide adenine dinucleotide, *Biochemistry 27*, 5082−5088.
37. Dalziel, K. (1963) Kinetic Studies of liver alcohol dehydrogenase and pH effects with coenzyme preparations of high purity, *J. Biol. Chem. 238*, 2850−2858.
38. Shore, J. D., Gutfreund, H., Brooks, R. L., Santiago, D., and Santiago, P. (1974) Proton equilibria and kinetics in the liver alcohol dehydrogenase reaction mechanism, *Biochemistry 13*, 4185−4191.
39. Kvassman, J., Larsson, A., and Pettersson, G. (1981) Substituent effects on the ionization step regulating desorption and catalytic oxidation of alcohols bound to liver alcohol dehydrogenase, *Eur. J. Biochem. 114*, 555−563.
40. Brooks, R. L., Shore, J. D., and Gutfreund, H. (1972) The effects of pH and temperature on hydrogen transfer in the liver alcohol dehydrogenase mechanism, *J. Biol. Chem. 247*, 2382−2383.
41. Deng, H., Schindler, J. F., Berst, K. B., Plapp, B. V., and Callender, R. (1998) A Raman spectroscopic characterization of bonding in the complex of horse liver alcohol dehydrogenase with NADH and *N*-cyclohexylformamide, *Biochemistry 37*, 14267−14278.
42. Kvassman, J., and Pettersson, G. (1979) Effect of pH on coenzyme binding to liver alcohol dehydrogenase, *Eur. J. Biochem. 100*, 115−123.
43. Kvassman, J., and Pettersson, G. (1978) Effect of pH on the process of ternary-complex interconversion in the liver-alcohol-dehydrogenase reaction, *Eur. J. Biochem. 87*, 417−427.
44. Sund, H., and Theorell, H. (1963) Alcohol Dehydrogenases, *The Enzymes 2nd Ed. 7*, 25−83.
45. Scharschmidt, M., Fisher, M. A., and Cleland, W. W. (1984) Variation of transition-state structure as a function of the nucleotide in reactions catalyzed by dehydrogenases. 1. Liver alcohol dehydrogenase with benzyl alcohol and yeast aldehyde dehydrogenase with benzaldehyde, *Biochemistry 23*, 5471−5478.
46. Shore, J. D., and Gutfreund, H. (1970) Transients in the reactions of liver alcohol dehydrogenase, *Biochemistry 9*, 4655−4659.
47. King, E. L., and Altman, C. (1956) A schematic method of deriving the rate laws for enzyme-catalyzed reactions, *J. Phys. Chem. 60*, 1375−1378.
48. Eklund, H., and Brändén, C.-I. (1987) Alcohol dehydrogenase, in *Biological Macromolecules and Assemblies: Vol. 3. Active Sites of Enzymes* (Jurnak, F. A., and McPherson, A., Eds.) pp 73−141, John Wiley & Sons, New York.
49. Rubach, J. K., and Plapp, B. V. (2002) Mobility of fluorobenzyl alcohols bound to liver alcohol dehydrogenases as determined by NMR and X-ray crystallographic studies, *Biochemistry 41*, 15770−15779.
50. Kim, C.-Y., Chang, J. S., Doyon, J. B., Baird, T. T., Jr., Fierke, C. A., Jain, A., and Christianson, D. W. (2000) Contribution of fluorine to protein-ligand affinity in the binding of fluoroaromatic inhibitors to carbonic anhydrase II, *J. Am. Chem. Soc. 122*, 12125−12134.
51. Hammes-Schiffer, S. (2002) Impact of enzyme motion on activity, *Biochemistry 41*, 13335−13343.
52. Cook, P. F., and Cleland, W. W. (1981) pH variation of isotope effects in enzyme-catalyzed reactions. 2. Isotope-dependent step not pH dependent. Kinetic mechanism of alcohol dehydrogenase, *Biochemistry 20*, 1805−1816.
53. Bahnson, B. J., Colby, T. D., Chin, J. K., Goldstein, B. M., and Klinman, J. P. (1997) A link between protein structure and enzyme catalyzed hydrogen tunneling, *Proc. Natl. Acad. Sci. U.S.A. 94*, 12797−12802.
54. Schmidt, J., Chen, J., DeTraglia, M., Minkel, D., and McFarland, J. T. (1979) Solvent deuterium isotope effect on the liver alcohol dehydrogenase reaction, *J. Am. Chem. Soc. 101*, 3634−3640.
55. Kvassman, J., and Pettersson, G. (1980) Unified mechanism for proton-transfer reactions affecting the catalytic activity of liver alcohol dehydrogenase, *Eur. J. Biochem. 103*, 565−575.
56. McFarland, J. T., and Chu, Y. H. (1975) Effect of pH on the liver alcohol dehydrogenase reaction, *Biochemistry 14*, 1140−1146.
57. Andersson, P., Kvassman, J., Lindström, A., Oldén, B., and Pettersson, G. (1981) Effect of NADH on the pK_a of zinc-bound water in liver alcohol dehydrogenase, *Eur. J. Biochem. 113*, 425−433.
58. Sideraki, V., Wilson, D. K., Kurz, L. C., Quiocho, F. A., and Rudolph, F. B. (1996) Site-directed mutagenesis of histidine 238 in mouse adenosine deaminase: substitution of histidine 238 does not impede hydroxylate formation, *Biochemistry 35*, 15019−15028.
59. Edwards, S. H., Thompson, D., Baker, S. F., Wood, S. P., and Wilton, D. C. (2002) The crystal structure of the H48Q active site mutant of human group IIA secreted phospholipase A2 at 1.5 Å resolution provides an insight into the catalytic mechanism, *Biochemistry 41*, 15468−15476.
60. Tu, C. K., Silverman, D. N., Forsman, C., Jonsson, B.-H., and Lindskog, S. (1989) Role of histidine 64 in the catalytic mechanism of human carbonic anhydrase II studied with a site-specific mutant, *Biochemistry 28*, 7913−7918.
61. Svensson, S., Strömberg, P., and Höög, J.-O. (1999) A novel subtype of class II alcohol dehydrogenase in rodents. Unique Pro-47 and Ser-182 modulates hydride transfer in the mouse enzyme, *J. Biol. Chem. 274*, 29712−29719.
62. Strömberg, P., Svensson, S., Berst, K. B., Plapp, B. V., and Höög, J.-O. (2004) Enzymatic mechanism of low-activity mouse alcohol dehydrogenase 2, *Biochemistry 43*, 1323−1328.

BI036103M